62 $(NH_2CH_2COOH)_2 \cdot HNO_3$

62A Pure compound

No. 62A-1 $(NH_2CH_2COOH)_2 \cdot HNO_3$, Diglycine nitrate

(M = 213.15)

1a Ferroelectricity in $(NH_2CH_2COOH)_2 \cdot HNO_3$ was discovered by Pepinsky et al. in 1958. 58Pep

b

phase	II	I	58Pep
state	F	P	
crystal system	monoclinic	monoclinic	
space group	$Pa-C_s^2$	$P2_1/a-C_{2h}^5$	
Θ [K]	206		

P_s makes an angle about 60° with the a axis in the (010) plane. 86Bar
$\rho_X = 1.580(5) \cdot 10^3$ kg m^{-3}. 68Sat
Transparent, colorless, deliquescent. 58Pep

2a Crystal growth: cooling or evaporation of aqueous solution [a]) and gel-growth method. [b]) [a]) 58Pep [b]) 81Pat

b Crystal form: Fig. 62A-1-001.

3a Unit cell parameters:
Phase I: a = 9.459(7) Å, b = 5.172(5) Å, c = 9.225(6) Å, β = 97.19(3)°, T = 295 K. 68Sat
Phase II: a = 9.485(8) Å, b = 5.132(5) Å, c = 9.089(7) Å, β = 97.89(4)°, T = 123 K. 68Sat

b Z = 2 in phases I and II. 68Sat
Crystal structure: Phase I: Table 62A-1-001, Table 62A-1-002; Fig. 62A-1-002.
Phase II: Table 62A-1-003, Table 62A-1-004; Fig. 62A-1-003, Fig. 62A-1-004.

4 Thermal expansion: Fig. 62A-1-005.

5a Dielectric constant: $\kappa_{[010]} = 9$, $\kappa_{[101]} = 14$, $\kappa_{[10\bar{1}]} = 20$ at RT. 58Pep
Anisotropy of dielectric constant in the (010) plane: Fig. 62A-1-006, Fig. 62A-1-007; see also 79Var
Curie-Weiss law in the direction parallel to P_s: 90Kha
$\kappa = \kappa_\infty + C/(T-\Theta_p)$, $T > \Theta_f$, with C = 860 K, κ_∞ = 15, f = 1 kHz.
Temperature dependence of $\kappa_{[101]}$: Fig. 62A-1-008.
Dielectric dispersion: Fig. 62A-1-009, Fig. 62A-1-010, Fig. 62A-1-011; see also 78Kol, 89Les
Low-frequency dielectric dispersion due to formation of polar clusters in phase I: see 94Shi
Effect of hydrostatic pressure: $[d\Theta_p/dp]_{p=0} = -4.1 \cdot 10^{-8}$ K Pa^{-1}. 73Ges
Effect of γ-irradiation: see Fig. 62A-1-035 in subsection 16.

b Nonlinear dielectric properties: Effect of E_{bias} on dielectrtic constant and polarization:
Fig. 62A-1-012, Fig. 62A-1-013.
$E = (1/\chi_p) P + \xi P^3 + \zeta P^5$ in phase I with $\xi = 5.7 \cdot 10^{12}$ V m^5 C^{-3}, $\zeta = 1.5 \cdot 10^{23}$ V m^9 C^{-5}. 84Igo1

c Spontaneous polarization: anisotropy in the (101) plane:
Fig. 62A-1-014, Fig. 62A-1-015.
Temperature dependence of spontaneous polarization and coercive field along the [101] direction: Fig. 62A-1-016, Fig. 62A-1-017.

	Effect of partial deuteration on the spontaneous polarization: see	89Kha
d	Pyroelectricity: see	82Gav
	Electrocaloric effect: Fig. 62A-1-018, Fig. 62A-1-019; see also	86Str2
6a	Heat capacity: Fig. 62A-1-020, Fig. 62A-1-021.	
	Effect of γ-irradiation: see Fig. 62A-1-036 in subsection 16.	
	Transition heat and transition entropy of the II-I transition: $\Delta Q_m = 9.6(4) \cdot 10^2$ J mol^{-1}, $\Delta S_m = 5.2(2)$ J K^{-1} mol^{-1}.	86Str2
7a	Piezoelectricity: Fig. 62A-1-022.	
8a	Elastic compliance: Fig. 62A-1-023;	
	see also	88Rod, 89Rod
	Longitudinal sound velocity and attenuation: Fig. 62A-1-024, Fig. 62A-1-025.	
9a	Orientation of optical indicatrix ellipsoid: Fig. 62A-1-026.	
	Birefringence: $\Delta n_X = 0.079$, $\Delta n_Y = 0.146$, $\Delta n_Z = 0.077$ at RT. $\lambda = 633$ nm.	82Var
	Temperature dependence of Δn_X: Fig. 62A-1-027.	
	Far infrared absorption: see	66Sat
c	Piezooptic effect: Fig. 62A-1-028.	
10a	Raman scattering: see	88Lav, 94Bar
13a	NMR: Fig. 62A-1-029, Fig. 62A-1-030, Fig. 62A-1-031.	
	NQR: Fig. 62A-1-032, Fig. 62A-1-033;	
	see also	87Rod
b	ESR of γ-ray irradiated and Cr^{3+}-doped crystals: see	73Oha, 88Bar
15b	Domain switching: Fig. 62A-1-034.	
	Low-frequency dielectric dispersion in phase II due to domain motion: see	83Bon
16	Radiation damage: effect of γ-ray irradiation: Fig. 62A-1-035, Fig. 62A-1-036;	
	see also	95Muk, 96Muk

Table 62A-1-001. $(NH_2CH_2COOH)_2 \cdot HNO_3$. Fractional coordinates and isotropic temperature parameters in phase I [68Sat]. $T = 295$ K. B is defined by Eq. (e) in Introduction.

	x	y	z	B [Å^2]
Glycine A *)				
N(1)	0.3483(9)	–0.0344(18)	0.1993(9)	2.01(15)
C(1)	0.2866(11)	0.1243(22)	0.3127(11)	2.05(18)
C(2)	0.1557(11)	–0.0035(22)	0.3632(11)	1.95(17)
O(1)	0.1076(8)	0.1127(17)	0.4662(8)	2.66(14)
O(2)	0.1042(8)	–0.1927(15)	0.2962(8)	2.25(13)
Glycine B' *)				
N(2)	0.3590(9)	–0.0427(18)	0.2126(9)	1.88(14)
C(3)	0.2983(10)	0.1015(21)	0.3291(10)	1.68(16)
C(4)	0.1612(10)	–0.0189(19)	0.3581(10)	1.34(15)
O(3)	0.0971(8)	0.1046(16)	0.4520(8)	2.36(13)
O(4)	0.1231(7)	–0.2326(15)	0.3049(7)	1.91(12)
Nitrate				
N(3)	0.0007(16)	0.0418(20)	0.0108(14)	2.22(16)
O(5)	0.0510(10)	0.2368(21)	0.0595(10)	3.97(19)
O(6)	–0.1095(13)	–0.0482(27)	0.0098(13)	6.13(28)
O(7)	0.1096(10)	–0.0805(20)	–0.0492(10)	3.77(18)

*) In phase I, a glycine ion takes two states A and B' in equal probability. The atomic coordinates of glycine B' are related to those of glycine B in Table 62A-1-003, Table 62A-1-004 by a symmetry operation 2_1.

Table 62A-1-002. $(NH_2CH_2COOH)_2 \cdot HNO_3$. Fractional coordinates and isotropic temperature parameters of hydrogen atoms in phase I [68Sat]. $T = 295$ K. B is defined by Eq. (e) in Introduction. The origin is taken at the midway of two a glide planes.

	x	y	z	B [Å^2]
Glycine A *)				
H(1)	0.3576(70)	0.1649(168)	0.3960(76)	2.87(115)
H(2)	0.2308(77)	0.3167(313)	0.2649(85)	4.36(142)
H(3)	0.2846(99)	–0.0926(191)	0.1344(65)	3.09(117)
H(4)	0.4170(50)	0.0714(164)	0.1409(66)	1.01(92)
H(5)	0.4211(50)	–0.1609(138)	0.2411(61)	0.92(84)
H(11)	0.0082(99)	–0.0006(429)	0.4817(79)	2.69(90)
Glycine B' *)				
H(6)	0.3819(70)	0.0565(211)	0.4320(76)	2.90(114)
H(7)	0.2827(55)	0.2987(149)	0.2922(62)	1.54(86)
H(8)	0.2773(113)	–0.1966(185)	0.1721(83)	4.42(142)
H(9)	0.3792(84)	0.1146(255)	0.1251(107)	4.18(143)
H(10)	0.4621(72)	–0.1331(243)	0.2646(88)	4.01(130)

*) See footnote of Table 62A-1-001.

Table 62A-1-003. $(NH_2CH_2COOH)_2 \cdot HNO_3$. Fractional coordinates and isotropic temperature parameters in phase II [68Sat]. $T = 123$ K. B is defined by Eq. (e) in Introduction.

	x	y	z	B [Å^2]
Glycine A				
N(1)	0.3454(11)	–0.0313(21)	0.2056(14)	0.87(18)
C(1)	0.2893(13)	0.1197(27)	0.3216(17)	1.17(23)
C(2)	0.1517(12)	–0.0004(24)	0.3606(15)	0.50(18)
O(1)	0.1009(9)	0.1218(18)	0.4640(11)	1.02(15)
O(2)	0.1012(10)	–0.1997(19)	0.2976(12)	1.31(16)
Glycine B				
N(2)	0.1401(10)	0.4613(22)	0.7903(13)	0.87(18)
C(3)	0.2011(12)	0.6126(24)	0.6790(15)	0.65(20)
C(4)	0.3363(12)	0.4816(26)	0.6384(16)	0.86(21)
O(3)	0.3972(9)	0.6073(17)	0.5423(11)	0.93(15)
O(4)	0.3775(8)	0.2780(17)	0.7020(10)	0.68(14)
Nitrate				
N(3)	0.0110(13)	0.0391(22)	0.0036(17)	1.23(19)
O(5)	0.0407(10)	0.2583(22)	0.0611(11)	1.48(16)
O(6)	–0.1112(11)	–0.0614(21)	0.0048(14)	1.83(18)
O(7)	0.1082(10)	–0.0823(20)	–0.0505(13)	1.53(17)

Table 62A-1-004. $(NH_2CH_2COOH)_2 \cdot HNO_3$. Fractional coordinates and isotropic temperature parameters of hydrogen atoms in phase II [68Sat]. $T = 123$ K. B is defined by Eq. (e) in Introduction.

	x	y	z	B [Å^2]
Glycine A				
H(1)	0.3699(56)	0.1021(142)	0.4216(72)	2.64(118)
H(2)	0.2591(51)	0.2889(115)	0.2885(52)	1.18(83)
H(3)	0.2655(41)	–0.0904(109)	0.1126(53)	1.06(85)
H(4)	0.4056(37)	0.0860(108)	0.1446(46)	0.12(82)
H(5)	0.4202(49)	–0.1780(103)	0.2411(59)	1.56(95)
H(11)	0.0151(44)	0.0300(93)	0.5029(64)	0.72(67)
Glycine B				
H(6)	0.1378(48)	0.5848(135)	0.5747(55)	0.83(78)
H(7)	0.2153(69)	0.7968(167)	0.7277(80)	3.89(145)
H(8)	0.2134(53)	0.3376(117)	0.8374(63)	1.73(90)
H(9)	0.1066(68)	0.6023(175)	0.8692(84)	3.39(126)
H(10)	0.0465(56)	0.3696(131)	0.7290(61)	2.08(99)

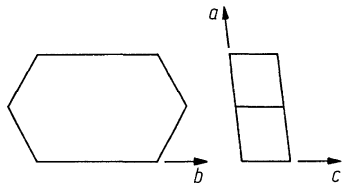

Fig. 62A-1-001. $(NH_2CH_2COOH)_2 \cdot HNO_3$. Crystal form [68Sat].

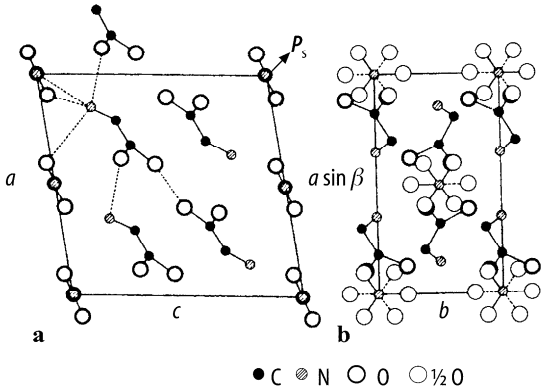

Fig. 62A-1-002. $(NH_2CH_2COOH)_2 \cdot HNO_3$. Structure of phase I [63Hos]. (**a**) Projection along the *b* axis, (**b**) projection along the *c* axis.

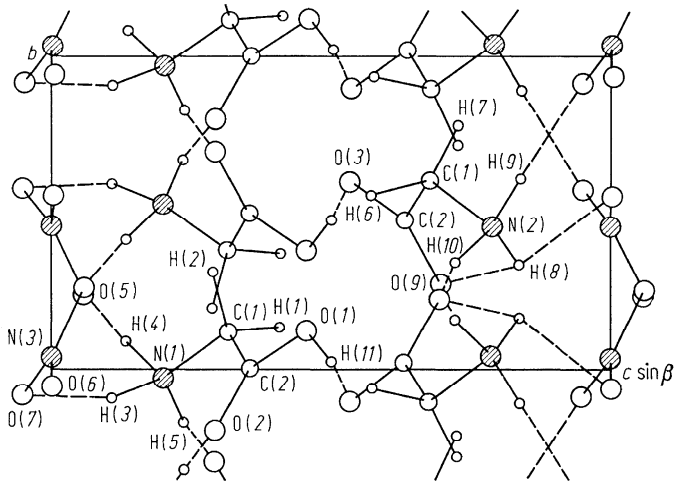

Fig. 62A-1-003. $(NH_2CH_2COOH)_2 \cdot HNO_3$. Structure of phase II [68Sat]. Projection along the *a* axis.

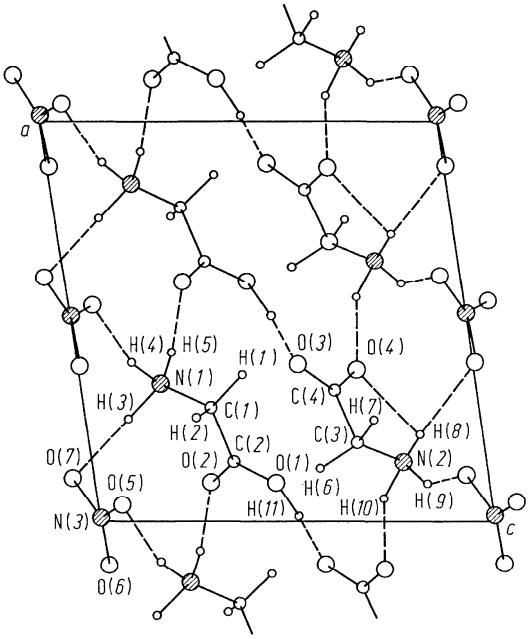

Fig. 62A-1-004. $(NH_2CH_2COOH)_2 \cdot HNO_3$. Structure of phase II [68Sat]. Projection along the *b* axis.

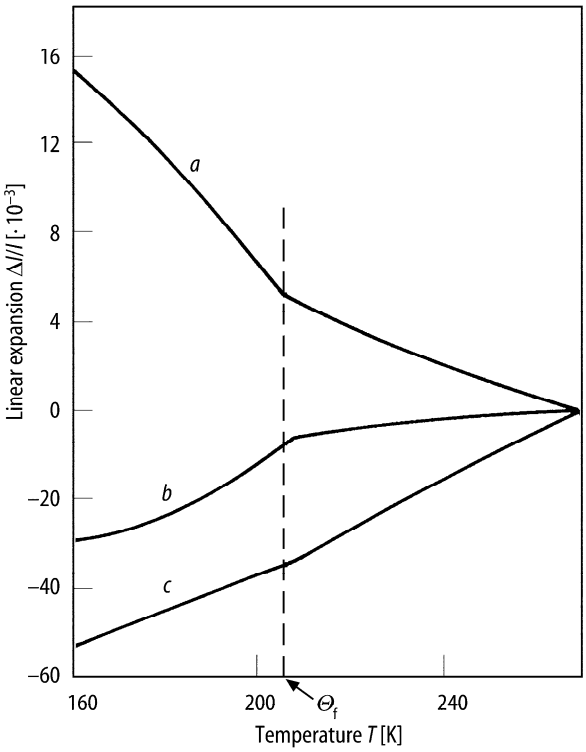

Fig. 62A-1-005. $(NH_2CH_2COOH)_2 \cdot HNO_3$. $\Delta l/l$ vs. T along three crystallographic axes [88Rod]. $\Delta l/l$: linear expansion. Note the scale for the *a* axis is different from others.

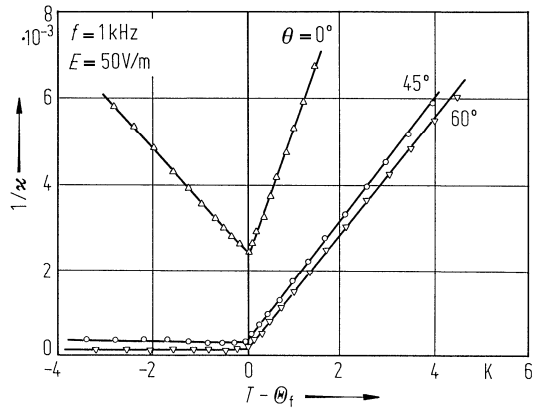

Fig. 62A-1-006. $(NH_2CH_2COOH)_2 \cdot HNO_3$. $1/\kappa$ vs. $T - \Theta_f$ [86Bar]. Parameter: θ. θ: angle between $\boldsymbol{E}$ and a axis in the (010) plane.

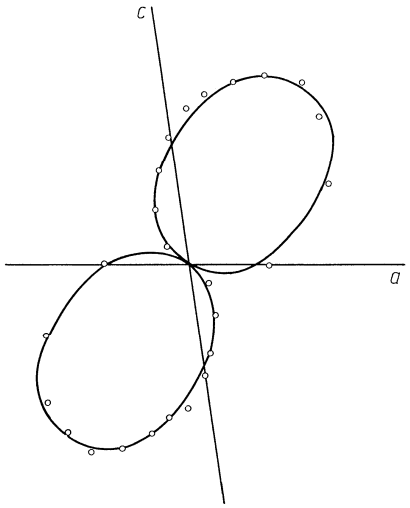

Fig. 62A-1-007. $(NH_2CH_2COOH)_2 \cdot HNO_3$. Anisotropy of κ in the (010) plane at $T = \Theta_f + 2$ K [86Bar].

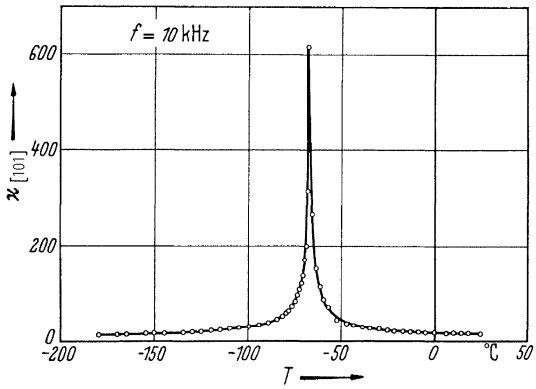

Fig. 62A-1-008. $(NH_2CH_2COOH)_2 \cdot HNO_3$. $\kappa_{[101]}$ vs. T [58Pep]. $\kappa_{[101]}$: dielectric constant along the [101] direction.

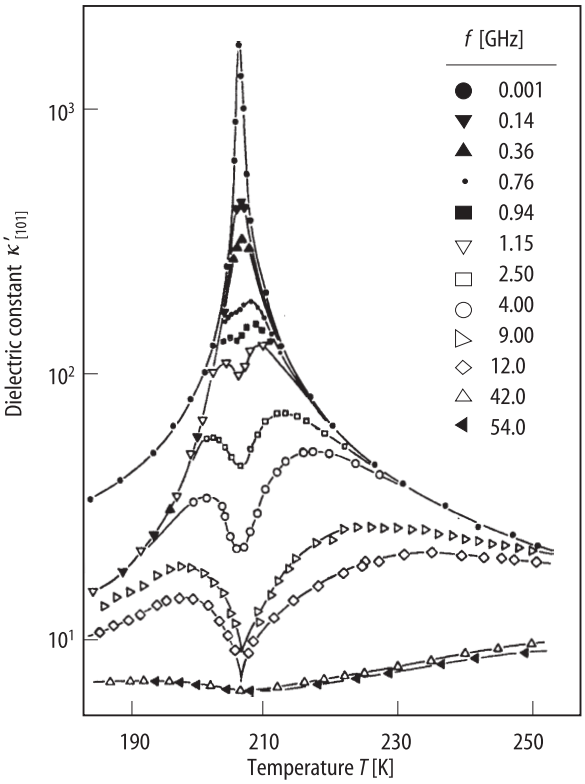

Fig. 62A-1-009. $(NH_2CH_2COOH)_2 \cdot HNO_3$. $\kappa'_{[101]}$ vs. T [89Sob]. Parameter: f. $\kappa'_{[101]}$: real part of dielectric constant along the [101] direction.

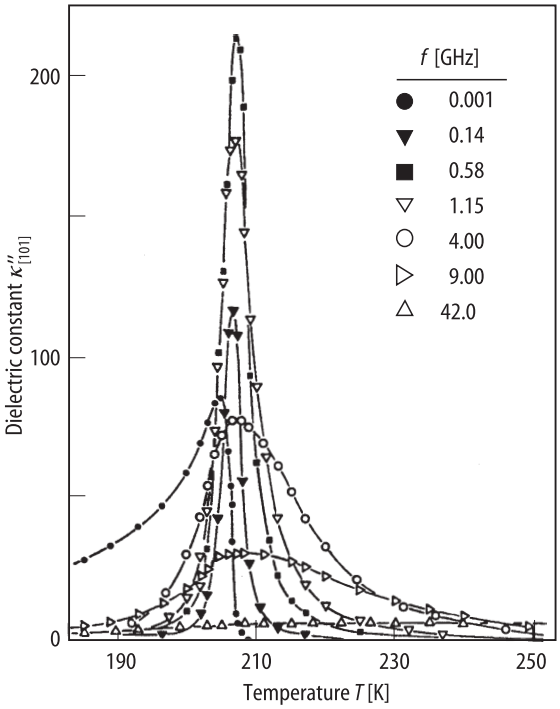

Fig. 62A-1-010. $(NH_2CH_2COOH)_2 \cdot HNO_3$. $\kappa''_{[101]}$ vs. T [89Sob]. Parameter: f. $\kappa''_{[101]}$: imaginary part of dielectric constant along the [101] direction.

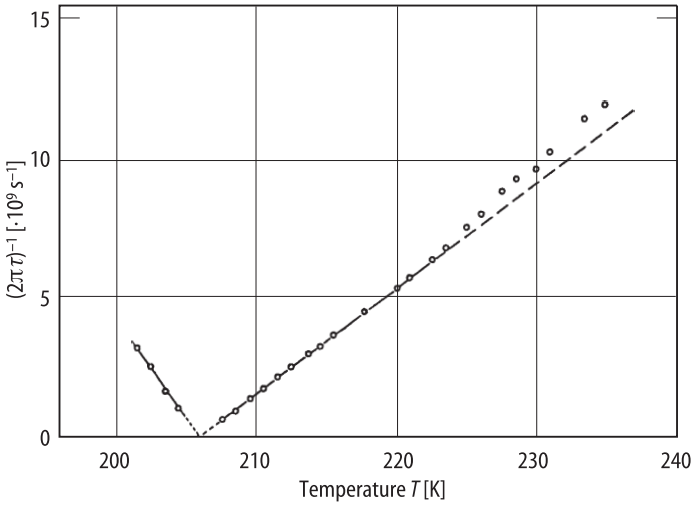

Fig. 62A-1-011. $(NH_2CH_2COOH)_2 \cdot HNO_3$. $1/(2\pi\tau)$ vs. T [89Sob]. τ: dielectric relaxation time.

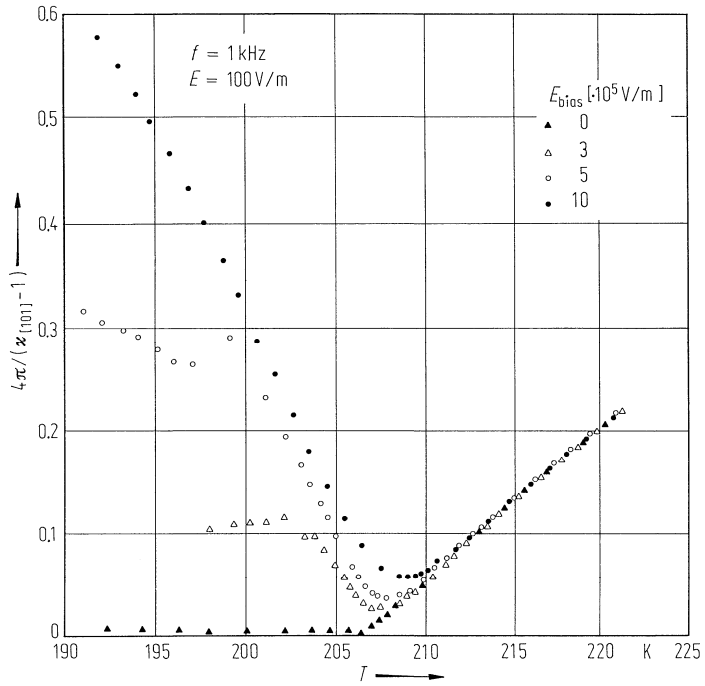

Fig. 62A-1-012. $(NH_2CH_2COOH)_2 \cdot HNO_3$. $4\pi/(\kappa_{[101]} - 1)$ vs. T [84Igo2]. Parameter: E_{bias}. $\kappa_{[101]}$: dielectric constant along the [101] direction.

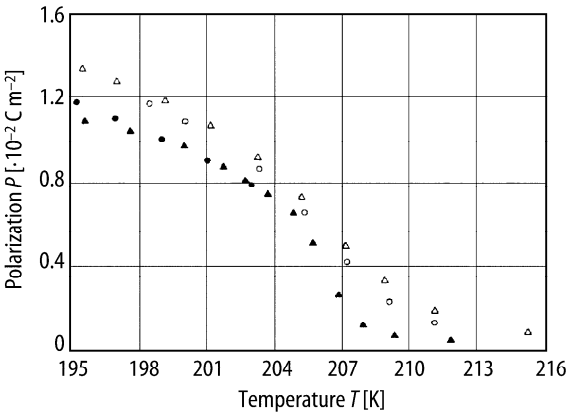

Fig. 62A-1-013. $(NH_2CH_2COOH)_2 \cdot HNO_3$. P vs. T [84Igo1]. Parameter: E. Solid circle: E = 0 kV/m, square: $E = 2 \cdot 10^2$ kV/m, open circle: $E = 8 \cdot 10^2$ kV/m, triangle: $E = 10 \cdot 10^2$ kV/m.

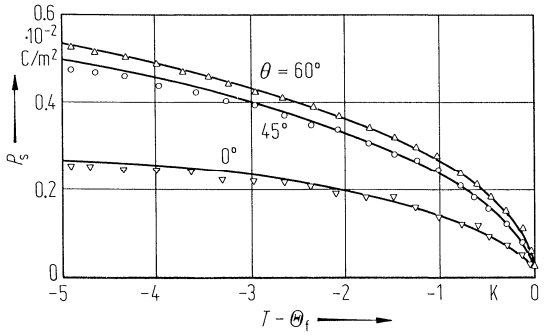

Fig. 62A-1-014. $(NH_2CH_2COOH)_2 \cdot HNO_3$. P_s vs. $T - \Theta_f$ [86Bar]. Parameter: θ. θ: angle between ***E*** and *a* axis in the (010) plane.

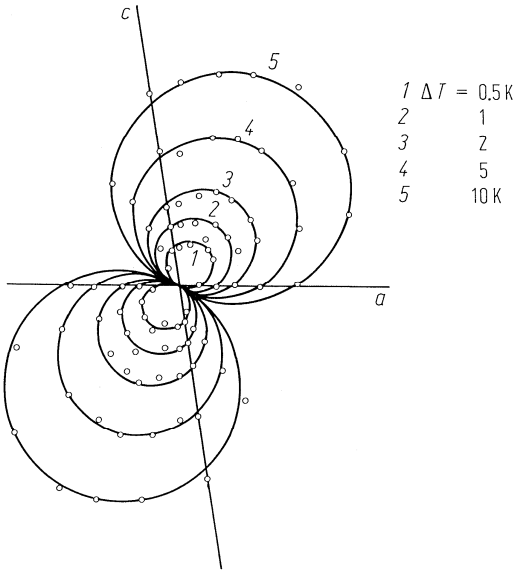

Fig. 62A-1-015. $(NH_2CH_2COOH)_2 \cdot HNO_3$. Anisotropy of P_s in the (010) plane [86Bar]. Parameter: $\Delta T = \Theta_f - T$.

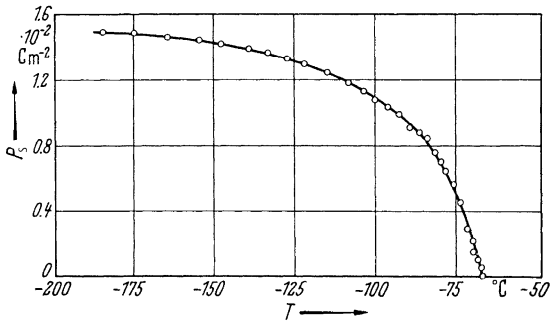

Fig. 62A-1-016. $(NH_2CH_2COOH)_2 \cdot HNO_3$. P_s vs. T [58Pep].

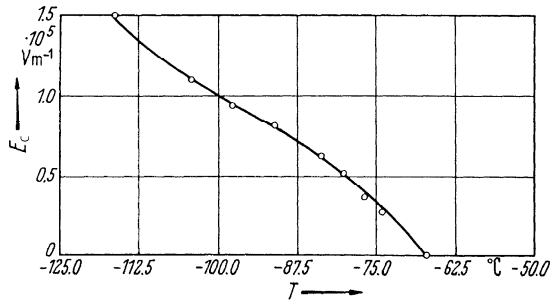

Fig. 62A-1-017. $(NH_2CH_2COOH)_2 \cdot HNO_3$. E_c vs. T [58Pep].

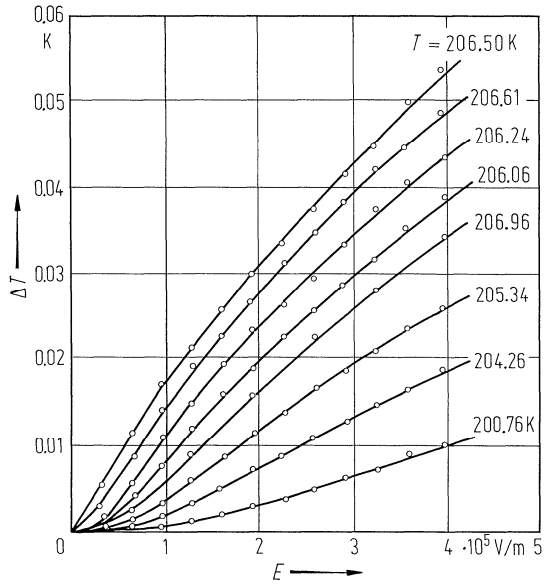

Fig. 62A-1-018. $(NH_2CH_2COOH)_2 \cdot HNO_3$. ΔT vs. E in the vicinity of Θ_f [86Str1]. Parameter: T. ΔT: change in temperature due to electrocaloric effect. E: external electric field.

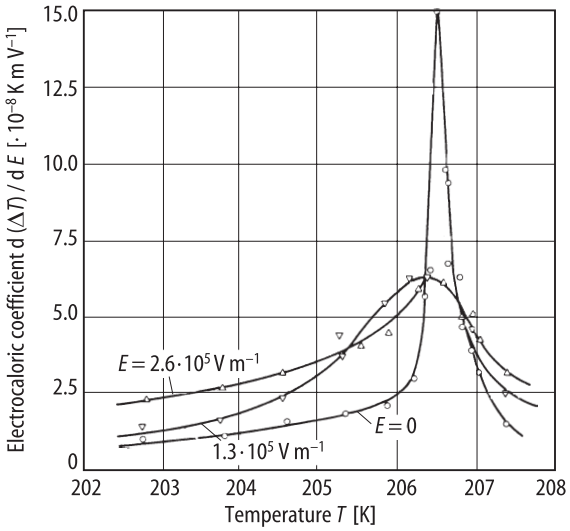

Fig. 62A-1-019. $(NH_2CH_2COOH)_2 \cdot HNO_3$. $d(\Delta T)/dE$ vs. T [86Str1]. Parameter: E. $d(\Delta T)/dE$: electrocaloric coefficient.

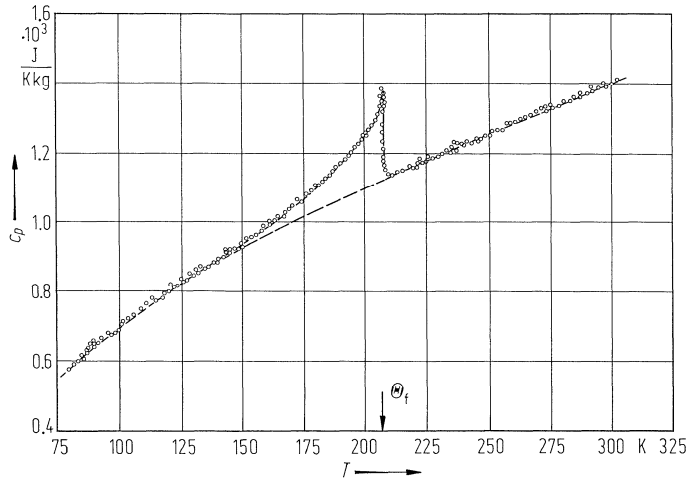

Fig. 62A-1-020. $(NH_2CH_2COOH)_2 \cdot HNO_3$. c_p vs. T [85Tar].

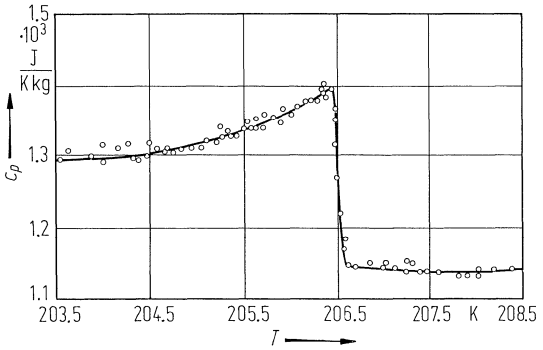

Fig. 62A-1-021. $(NH_2CH_2COOH)_2 \cdot HNO_3$. c_p vs. T in the vicinity of Θ_f [85Tar].

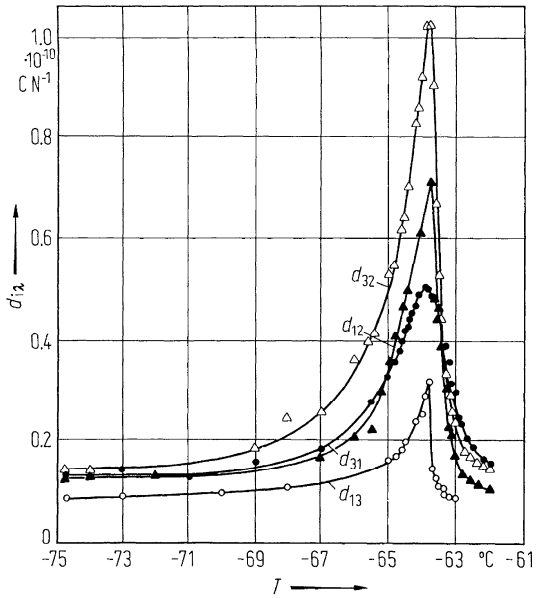

Fig. 62A-1-022. $(NH_2CH_2COOH)_2 \cdot HNO_3$. $d_{i\lambda}$ vs. T [79Var].

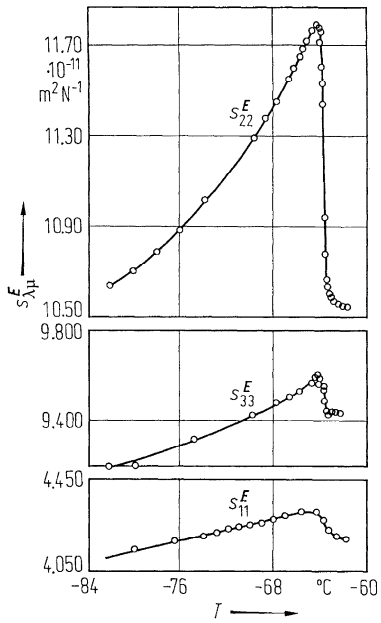

Fig. 62A-1-023. $(NH_2CH_2COOH)_2 \cdot HNO_3$. $s^E_{\lambda\mu}$ vs. T [79Var].

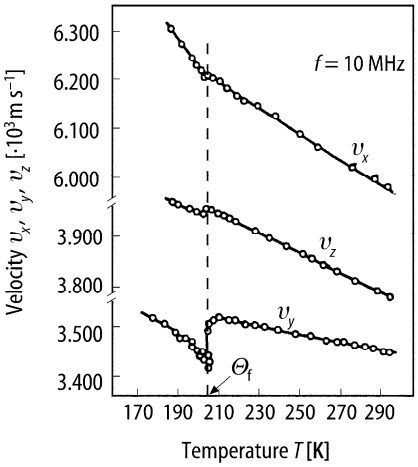

Fig. 62A-1-024. $(NH_2CH_2COOH)_2 \cdot HNO_3$. v_i vs. T [88Str]. v_i: velocity ot the longitudinal sound propagating in the i direction. For the relation between the coordinate system and the crystallographic axes: see Fig. 62A-1-026.

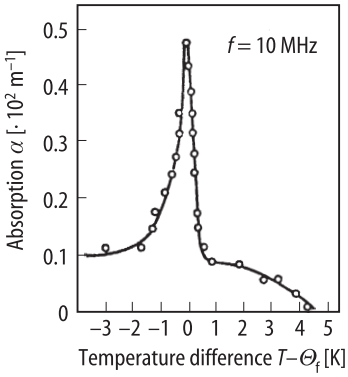

Fig. 62A-1-025. $(NH_2CH_2COOH)_2 \cdot HNO_3$. α vs. $T-\Theta_f$ [88Str]. α: absorption coefficient of the longitudinal sound propagating along the b axis.

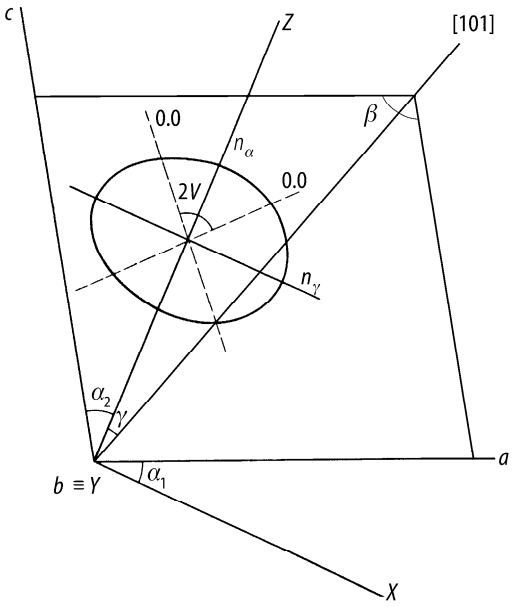

Fig. 62A-1-026. $(NH_2CH_2COOH)_2 \cdot HNO_3$. Crystallographic orientation of optical indicatrix at 295 K [82Var]. $\alpha_1 = 25.4(5)°$, $\alpha_2 = 33.2(5)°$, $\beta = 97.8(5)°$, $\gamma = 17.2(5)°$, $2V = 86(1)°$.

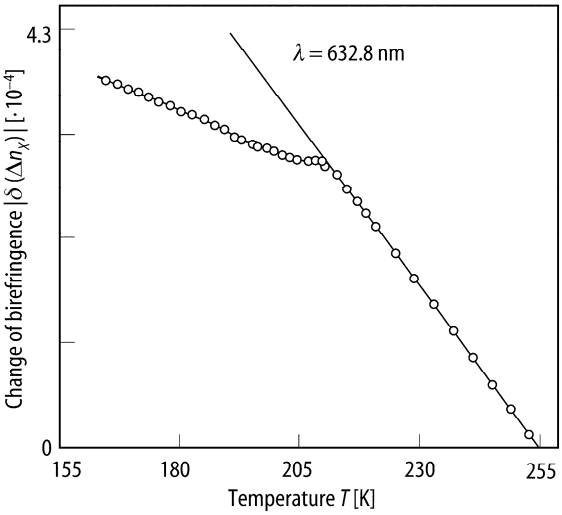

Fig. 62A-1-027. $(NH_2CH_2COOH)_2 \cdot HNO_3$. $|\delta(\Delta n_X)|$ vs. T [91Kos]. $\delta(\Delta n_X)$: change of birefringence.

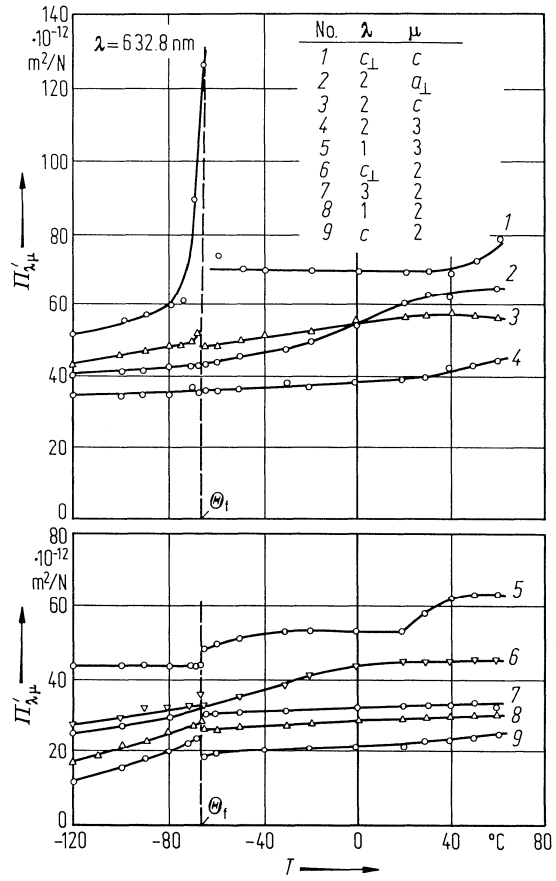

Fig. 62A-1-028. $(NH_2CH_2COOH)_2 \cdot HNO_3$. $\Pi'_{\lambda\mu}$ vs. T [82Rom]. $\Pi'_{\lambda\mu}$: piezooptic constants. $\Pi'_{\lambda\mu} \equiv \Pi'_{(ij)\mu} = n_i^3 \Pi_{i\mu} - n_j^3 \Pi_{j\mu}$, $i \neq \lambda$, $j \neq \lambda$. Crystal optic axes X, Y, Z are denoted by 1, 2, 3, respectively (see Fig. 62A-1-026). $a_\perp$ and $c_\perp$ are directions perpendicular to the ab and cb plane, respectively.

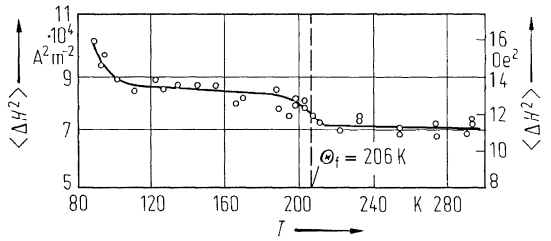

Fig. 62A-1-029. $(NH_2CH_2COOH)_2 \cdot HNO_3$. $\langle \Delta H^2 \rangle$ vs. T [70Bli]. $\langle \Delta H^2 \rangle$: second moment of proton NMR line.

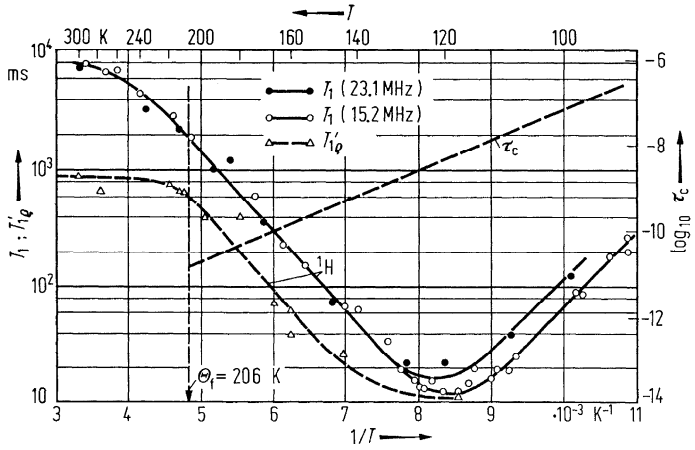

Fig. 62A-1-030. $(NH_2CH_2COOH)_2 \cdot HNO_3$. T_1, $T'_{1\rho}$, $\log_{10} \tau_c$ vs. $1/T$ [70Bli]. $T'_{1\rho}$: dipolar spin-lattice relaxation time in rotating frame, τ_c : correlation time [s].

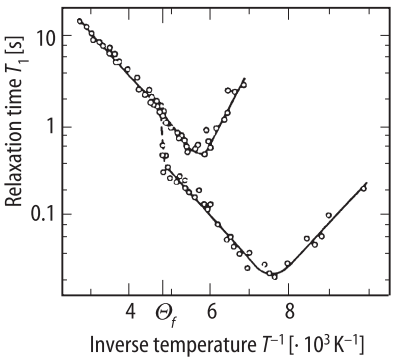

Fig. 62A-1-031. $(NH_2CH_2COOH)_2 \cdot HNO_3$. T_1 vs. $1/T$ [89Kot]. T_1: proton spin lattice relaxation time.

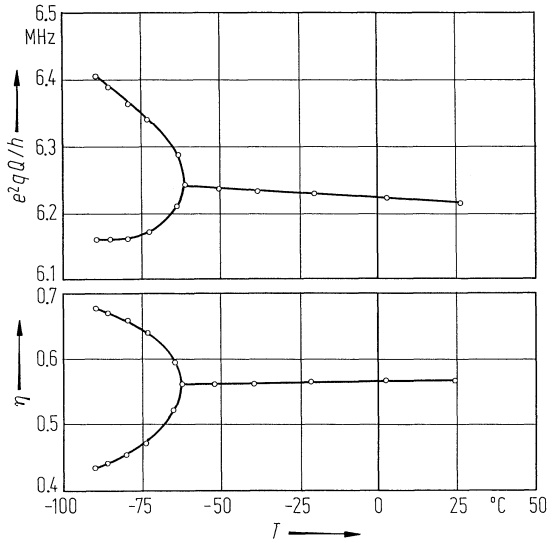

Fig. 62A-1-032. $(NH_2CH_2COOH)_2 \cdot HNO_3$. e^2qQ/h, η vs. T [86Sel]. e^2qQ/h: ^{17}O quadrupole coupling constant, η: asymmetry parameter.

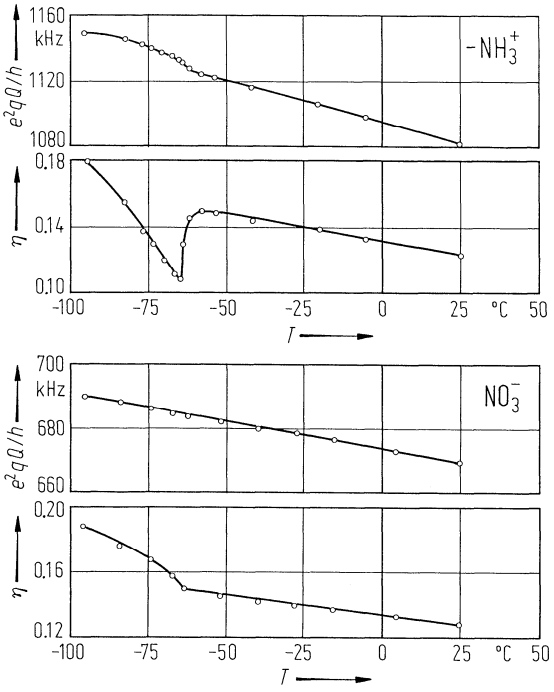

Fig. 62A-1-033. $(NH_2CH_2COOH)_2 \cdot HNO_3$. e^2qQ/h, η vs. T [86Sel]. e^2qQ/h: ^{14}N quadrupole coupling constant, η: asymmetry parameter.

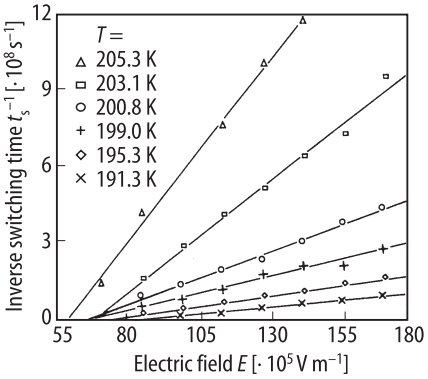

Fig. 62A-1-034. $(NH_2CH_2COOH)_2 \cdot HNO_3$. $1/t_s$ vs. E [90Maj]. Parameter: T. t_s: domain switching time.

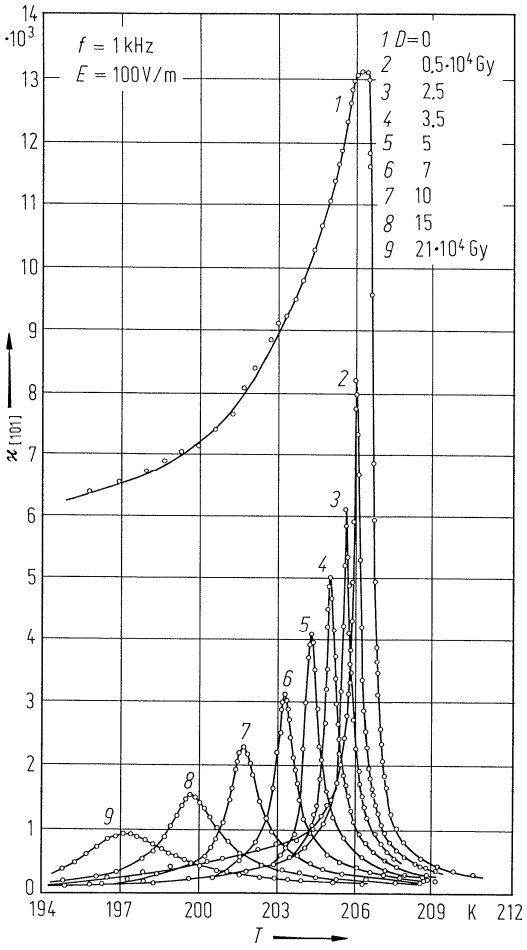

Fig. 62A-1-035. $(NH_2CH_2COOH)_2 \cdot HNO_3$. $\kappa_{[101]}$ vs. T [87Yur]. Parameter: D. $\kappa_{[101]}$: dielectric constant along the [101] direction, D: γ-ray irradiation dose.

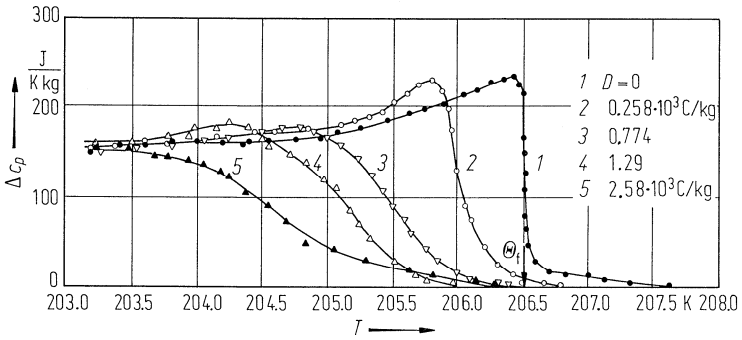

Fig. 62A-1-036. $(NH_2CH_2COOH)_2 \cdot HNO_3$. Δc_p vs. T [86Str2]. Parameter: D. Δc_p: anomalous part of specific heat capacity at constant pressure, D: γ-ray irradiation dose.

References

58Pep Pepinsky, R., Vedam, K., Hoshino, S., Okaya, Y.: Phys. Rev. **111** (1958) 430.
63Hos Hoshino, S., Sato, S., Toyoda, K.: Jpn. J. Appl. Phys. **2** (1963) 519.
66Sat Sato, Y.: J. Chem. Phys. **45** (1966) 275.
68Sat Sato, S.: J. Phys. Soc. Jpn. **25** (1968) 185.
70Bli Blinc, R., Jamsek-Vilfan, M., Lahajnar, G., Hajukovic, G.: J. Chem. Phys. **52** (1970) 6407.
73Ges Gesi, K., Ozawa, K.: Jpn. J. Appl. Phys. **12** (1973) 951.
73Oha Ohashi, S., Abe, R., Kawamura, A.: J. Phys. Soc. Jpn. **34** (1973) 1694.
78Kol Kolodziej, H.A., Narewski, E., Sobczyk, L.: Acta Phys. Polon. A **53** (1978) 79.
79Var Varikash, V.M., Rodin, S.V.: Kristallografiya **24** (1979) 383; Sov. Phys. Crystallogr. (English Transl.) **24** (1979) 221.
81Pat Patel, G.M.: J. Cryst. Growth **54** (1981) 602.
82Gav Gavrilova, N.D., Varikash, V.M., Rodin, S.V., Galygin, A.N.: Fiz. Tverd. Tela **24** (1982) 2183; Sov. Phys. Solid State (English Transl.) **24** (1982) 1243.
82Rom Romanyuk, N.A., Myutsyk, B.G.: Ukrain. Fiz. Zh. **27** (1982) 1206.
82Var Varikash, V.M., Romanyuk, N.A., Mytsyk, B.G.: Zh. Prikl. Spektrosk. **37** (1982) 319; J. Appl. Spectrosc. (English Transl.) **37** (1982) 977.
83Bon Bondarenko, V.V., Varikash, V.M., Gridnev, S.A., Shuvalov, L.A.: Izv. Akad. Nauk SSSR, Ser. Fiz. **47** (1983) 825; Bull. Acad. Sci. USSR, Phys. Ser. (English Transl.) **47**, No. 4 (1983) 199.
84Igo1 Igoshin, I.P.: Fiz. Tverd. Tela **26** (1984) 985; Sov. Phys. Solid State (English Transl.) **26** (1984) 602.
84Igo2 Igoshin, I.P., Gradkii, V.V., Kirikov, V.A.: Fiz. Tverd. Tela **26** (1984) 3688; Sov. Phys. Solid State (English Transl.) **26** (1984) 2220.
85Tar Taraskin, S.A., Savilova, Z.V., Strukov, B.A., Varikash, V.M.: Izv. Akad. Nauk SSSR, Ser. Fiz. **49** (1985) 268; Bull. Acad. Sci. USSR, Phys. Ser. (English Transl.) **49**, No. 2 (1985) 50.
86Bar Baranov, A.I., Khasinevich, N.I., Rodin, S.V.: Kristallografiya **31**(1986) 501; Sov. Phys. Crystallogr. (English Transl.) **31** (1986) 295.
86Sel Seliger, J., Zagar, V., Blinc, R., Novak, A., Rodin, S.: Ferroelectrics Lett. **6** (1986) 93.
86Str1 Strukov, B.A., Savilova, Z.V., Taraskin, S.A., Varikash, V.M.: Fiz. Tverd. Tela **28** (1986) 733; Sov. Phys. Solid State (English Transl.) **28** (1986) 408.
86Str2 Strukov, B.A., Taraskin, S.A., Savilova, Z.V.: Phys. Status Solidi (a) **95** (1986) 447.
87Rod Rodin, S.V., Seliger, J., Blinc, R., Zagar, V.: Fiz. Tverd. Tela **29** (1987) 1871; Sov. Phys. Solid State (English Transl.) **29** (1987) 1076.
87Yur Yurin, V.A., Igoshin, I.P., Zheludev, I.S.: Ferroelectrics **73** (1987) 383.
88Bar Barb, D., Grecu, N.M., Zheludev, V.S., Yurin, V.A., Igoshin, I.P.: Rev. Roum. Phys. **33** (1988) 375.
88Lav Lavrencic, B.B., Rodin, S.V.: Ferroelectrics **88** (1988) 37.
88Rod Rodin, S.V., Zgonik, M., Copic, M.: Ferroelectrics **82** (1988) 85.
88Str Strukov, B.A., Rodin, S.V., Minaeva, K.A., Lenchik, I.A.: Fiz. Tverd. Tela **30** (1988) 810; Sov. Phys. Solid State (English Transl.) **30** (1988) 464.
89Kha Khasinevich, N.I., Rodin, S.V., Andreev, E.F.: Fiz. Tverd. Tela **31** (1989) 275; Sov. Phys. Solid State (English Transl.) **31** (1989) 1073.
89Kot Kotelevets, A.M., Pogrebnyak, S.V., Khasinevich, N.I., Chesnokov, E.D.: Kristallografiya **34** (1989) 1169; Sov. Phys. Crystallogr. (English Transl.) **34** (1989) 705.
89Les Leshchenko, M.A., Poplavko, Yu.M., Bovtun, V.P., Igoshin, I.P., Yurin, V.A.: Fiz. Tverd. Tela **31** (1989) 286; Sov. Phys. Solid State (English Transl.) **31** (1989) 157.
89Rod Rodin, S.V., Zgonik, M., Copic, M.: Kristallografiya **34** (1989) 505; Sov. Phys. Crystallogr. (English Transl.) **34** (1989) 303.
89Sob Sobiestianskas, R., Grigas, J., Czapla, Z.: Ferroelectrics **100** (1989) 187.
90Kha Khasinevich, N.I., Varikash, V.M., Rodin, S.V., Baranov, A.I.: Ferroelectrics **103** (1990) 1.
90Maj Majszczyk, J., Dacko, S., Czapla, Z.: Ferroelectrics **111** (1990) 185.
91Kos Kosurek, B., Przeslawski, I., Czapla, Z.: Izv. Alad. Nauk SSSR, Ser. Fiz. **55** (1991) 512; Bull Acad. Sci. USSR, Phys. Ser. (English Transl.) **55**, No. 3 (1991) 91.

94Bar Baran, J., Barnes, A.J., Ratajczak, K.H.: J. Mol. Struct. **325** (1994) 71.
94Shi Shil'nikov, A.V., Nadolinskaya, E.G., Fedorikhin, V.A., Rodin, S.V.: Kristallografiya **39** (1994) 84; Crystallogr. Rep. (English Transl.) **39** (1994) 74.
95Muk Mukhtarov, N., Yushin, N.K.: Pis'ma Zh. Tekh. Fiz. **21** (1995) 39; Tech. Phys. Lett. (English Transl.) **21** (1995) 879.
96Muk Mukhtarov, N., Yushin, N.K.: Ferroelectrics Lett. **21** (1996) 135.